British Geological Survey
NATURAL ENVIRONMENT RESEARCH COUNCIL

Cathodoluminescence petrography and fluid inclusion microthermometry of vein calcites from Laxemar borehole KLX-01, Sweden.

Environmental Protection Programme

Commissioned Report CR/04/161

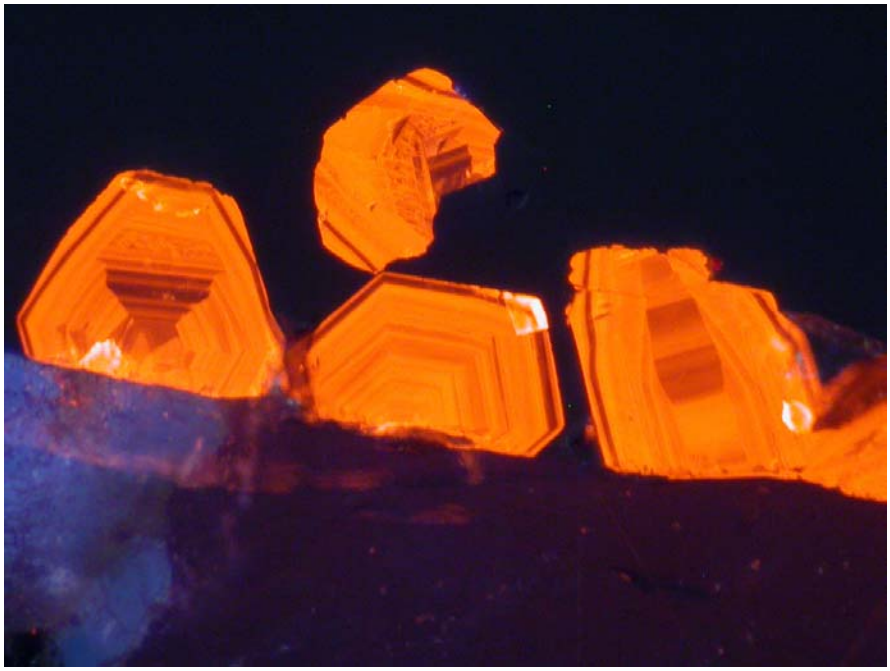

BRITISH GEOLOGICAL SURVEY

COMMISSIONED REPORT CR/04/161

Cathodoluminescence petrography and fluid inclusion microthermometry of vein calcites from Laxemar borehole KLX-01, Sweden.

JE Bouch

Key words

Laxemar, Calcite, Fluid Inclusions, Cathodoluminescence, Fluid Chemistry.

Front cover

Cathodoluminescence image of sector and growth zoned calcite euhedra resting on a fracture surface. Sample MPLJ538, 153.50 m bGL, Field of view 1 mm.

Bibliographical reference

BOUCH, J.E.. 2004. Cathodoluminescence petrography and fluid inclusion microthermometry of vein calcites from Laxemar borehole KLX-01, Sweden.. *British Geological Survey Commissioned Report*, CR/04/161. 20pp.

Keyworth, Nottingham British Geological Survey 2004

BRITISH GEOLOGICAL SURVEY

The full range of Survey publications is available from the BGS Sales Desks at Nottingham and Edinburgh; see contact details below or shop online at www.thebgs.co.uk

The London Information Office maintains a reference collection of BGS publications including maps for consultation.

The Survey publishes an annual catalogue of its maps and other publications; this catalogue is available from any of the BGS Sales Desks.

The British Geological Survey carries out the geological survey of Great Britain and Northern Ireland (the latter as an agency service for the government of Northern Ireland), and of the surrounding continental shelf, as well as its basic research projects. It also undertakes programmes of British technical aid in geology in developing countries as arranged by the Department for International Development and other agencies.

The British Geological Survey is a component body of the Natural Environment Research Council.

Keyworth, Nottingham NG12 5GG

☎ 0115-936 3241 Fax 0115-936 3488
e-mail: sales@bgs.ac.uk
www.bgs.ac.uk
Shop online at: www.thebgs.co.uk

Murchison House, West Mains Road, Edinburgh EH9 3LA

☎ 0131-667 1000 Fax 0131-668 2683
e-mail: scotsales@bgs.ac.uk

London Information Office at the Natural History Museum (Earth Galleries), Exhibition Road, South Kensington, London SW7 2DE

☎ 020-7589 4090 Fax 020-7584 8270
☎ 020-7942 5344/45 email: bgslondon@bgs.ac.uk

Forde House, Park Five Business Centre, Harrier Way, Sowton, Exeter, Devon EX2 7HU

☎ 01392-445271 Fax 01392-445371

Geological Survey of Northern Ireland, 20 College Gardens, Belfast BT9 6BS

☎ 028-9066 6595 Fax 028-9066 2835

Maclean Building, Crowmarsh Gifford, Wallingford, Oxfordshire OX10 8BB

☎ 01491-838800 Fax 01491-692345

Parent Body

Natural Environment Research Council, Polaris House, North Star Avenue, Swindon, Wiltshire SN2 1EU

☎ 01793-411500 Fax 01793-411501
www.nerc.ac.uk

Foreword

This report is the published product of a study by the British Geological Survey (BGS) and presents results and interpretations derived from cathodoluminescence and fluid inclusion microthermometric analysis of fracture-lining calcite in samples from Laxemar borehole KLX-01. The work was undertaken on behalf of Terralogica AB and the Swedish Nuclear Waste Management company (SKB) as part of the Palaeohydrogeological Data Analysis and Model Testing (PADAMOT) project funded as part of the Framework Five programme of the European Union.

Contents

FIGURES

PLATES

TABLES

Summary

This report provides results and interpretations of the cathodoluminescence (CL) and fluid inclusion microthermometric properties of fracture-filling calcite cements from the Swedish Nuclear Waste Management company (SKB) Laxemar-01 borehole (KLX-01). The work was undertaken on behalf of Terralogica AB as part of the Palaeohydrogeological Data Analysis and Model Testing (PADAMOT) project funded as part of the Framework Five programme of the European Union.

CL imaging has allowed the recognition of five calcite generations which show evidence for significant fracture rejuvenation, reworking, brecciation, replacement and cementation by later calcite generations. These generations are consistent with those recognised during earlier work. which on this borehole. Fluid inclusion microthermometric data has been acquired from all the generations.

The fluids are shown to have variable chemistries, with relatively low-salinity (brackish water, typically <2 wt% $CaCl_2$ equiv.) inclusions occurring in close proximity to very saline solutions (up to 24 wt% $CaCl_2$ equiv.), even within the same calcite generation. The higher salinity inclusions are NaCl-$CaCl_2$-H_2O brines, with high $CaCl_2$ / (NaCl+$CaCl_2$) ratios inferred for the highest salinity inclusions. The chemical species present in the relatively low salinity inclusions are unknown.

The presence of high salinity fluids even at shallow depths in the borehole (well within the present day freshwater zone that extents down to approximately 1000 m), indicates that the transition zone between the fresh and saline fluids was closer to ground level at some time during precipitation of these cements. Similarly the absence of fresh water inclusions below approximately 840 m, suggests that the transition zone was never much deeper than 840 m during calcite precipitation.

Some, apparently systematic, variations in fluid chemistry are evident between the calcite generations but interpretation is hindered by the difficulty in distinguishing between primary and secondary inclusions due to the altered nature of the earlier generations.

1 Introduction

This report presents analytical results and interpretations based upon the cathodoluminescence (CL) and fluid inclusion microthermometric analysis of a suite of samples from the SKB KLX-01 borehole. The samples are subset of the samples collected by E-L Tullborg (Terralogica AB), A.E. Milodowski and M. Gillespie (BGS) during fracture logging of KLX-01 in March 2003. Equivalent polished sections of many of the samples have been previously imaged using CL in support of ion-microprobe analyses (in progress at Edinburgh University). All depths quoted are in m below ground level (m bGL). The samples are from two distinct intervals within the borehole: 13-255 m and 840-950 m.

Table 1 List of samples from KLX-01 analysed during this study.

Sample	Depth (m)	Supporting EPMA Microchemical Maps [2]	Duplicate Standard Polished Thin Section	CL imaging (This Study)	Calcite Generations Present [1]	Fluid Inclusion Prospectivity	Fluid Inclusion Microthermometry	Number of Inclusions in Calcite with Data
MPLJ522	13.10		Y	Y	3	Poor	-	-
MPLJ523	13.95	Y	Y [2]	Y	3b, 3c, 3d, 4?	Good	Y	19
MPLJ527	37.35		Y	Y	2, 3b?, 3d?	Moderate	-	-
MPLJ529	51.30		Y	Y	2, 3b, 3d	Good	Y	20
MPLJ532	60.00	Y	Y [2]	Y	2, 3b?, 3c? 3d	Moderate	-	-
MPLJ538	153.50	Y	Y [2]	Y	3a	Moderate	Y	0
MPLJ546	189.90		Y	Y	2, 3a, 3b, 3d	Good	Y	25
MPLJ549	223.90	Y	Y [2]	Y	2, 3a, 3b	Moderate	Y	6
MPLJ551	255.00		Y	Y	unknown	Poor	-	-
MPLJ554	840.00	Y	Y [2]	Y	3a, 3c, 3d	Good	Y	17
MPLJ557	936.80	Y	Y [2]	Y	2?, 3a?, 3c, 3d	Moderate	-	-
MPLJ558	939.00		Y	Y	2?, 3a, 3b, 3c,3d	Moderate	Y	13
MPLJ559	945.34		Y	Y	2?, 3a, 3b, 3c,3d	Poor	-	-
						TOTAL		100

[1] Calcite generation is a refinement of that presented by Milodowski *et al.* (1998a; Table 2). See results section for further details.

[2] Denotes samples with supporting EPMA microchemical maps obtained from counterpart polished thin-sections.

1.1 BACKGROUND

A summary of geological events and mineralisation history for the Äspö and Laxemar area is given in Table 3. Within the context of this overall history, Milodowski *et al.* (1998a) were able to distinguish 4 generations of calcite (Table 2). The morphological variations in the last two generations (Calcites 3 and 4) follow a similar pattern to that seen at Sellafield (Milodowski *et al.* 1998b) with c-axis flattened ("nailhead") morphologies in the shallowest samples, and progressively more c-axis elongated ("scalenohedral" of "acute rhombohedral") forms at greater depth. These variations were cautiously interpreted by Milodowski *et al.* (1998a) to relate to changes in groundwater salinity with depth.

The aim of this work was to collect fluid inclusion microthermometric data from the youngest generations of calcite in samples from KLX-01, in order to provide more detailed constraints on temperatures and groundwater chemistry during calcite formation than have been available previously.

1.2 ANALYTICAL METHODS

A detailed description of the methodology employed is given in Appendix 3. However, in summary:

- Following screening to identify workable inclusions, fluid inclusion microthermometry was undertaken on "regions of interest" extracted from doubly-polished fluid inclusion wafers.
- CL analysis prior to fluid inclusion analysis would have been a useful aid in the targeting of specific calcite generations for analysis. However, CL analysis causes significant heating of the sample that may cause inclusions to leak or decrepitate. Consequently, in order to get the best possible thermometric data, microthermometry was performed prior to the CL imaging, meaning that at the time of analysis the cement generation within which an inclusion occurs could not be determined.
- Attempts were made to collect temperatures of homogenisation (T_h for liquid + vapour bearing inclusions only), first ice melting (T_{fm}), final ice melting (T_{ice}) and hydrohalite melting (T_{hyd}).
- CL imaging of the analysed regions of interest was undertaken retrospectively and the calcite generation containing the analysed inclusions were identified (using a refinement of the paragenetic scheme established by Milodowski *et al.* (1998a; Table 2 and Table 4).

CL petrographical descriptions and images of the fracture fills, showing the positions of the analysed inclusions are presented in Appendix 1, and a complete listing of the fluid inclusion data, including coding of inclusions by calcite generation is presented in Appendix 2.

Table 2 Summary of the calcite cement generations recognised by Milodowski et al. (1998a).

	Description	Timing
1	Bright yellow luminescence. Predates a late phase of quartz, local laumonite mineralisation, and is deformed by later fracturing and shearing.	Either related to the later stages of hydrothermal circulation associated with the Götemar Granite (Event 4 in Table 3) or a 1100 Ma regional low-temperature burial metamorphic event (Event 5).
2	Moderate- to weak- brown-orange luminescence. Postdates laumonite mineralisation and dissolution of earlier-formed epidote. This calcite is commonly deformed, brecciated, disrupted with most pronounced shearing observed in samples from below 800 m in the Laxemar boreholes.	There is evidence for corrosion of Calcite 2, prior to syntaxial overgrowth by Calcite 3. Calcite 2 may relate to fracturing and mineralisation during post-Caledonian deep burial (Event 6 in Table 3).
3	Weakly-luminescent, and forms euhedral overgrowths on earlier calcite with some relationship observed between morphology and present day groundwater chemistry, suggesting this calcite formed as part of Event 7 (Table 3).	In many of the samples studies by Milodowski *et al.* (1998a) this is the youngest calcite generation observed. Interpreted to be quaternary or recent in age.
4	Bright yellow luminescent, forming euhedral overgrowths on earlier Calcite 2/3, with morphological variations also reflecting the present day groundwater chemistry.	Interpreted to be quaternary or recent in age.

Table 3 Sequence of events and fracture mineralisation history for Äspö and Laxemar (after Tullborg 1995).

Event	Effect/Mineralisation	Comment
0	Formation of the Äspö Granitoids	c. 1800 Ma
1	Regional deformation	1660-1400 Ma
2	Mylonitisation; formation of fine-grained epidote, muscovite and quartz recrystallisation.	Some mylonites probably belong to last phase of event 2.
3	Reactivation of mylonites and formation of idiomorphic epidote and fluorite.	Intrusion of the anorogenic Götemar Intrusion c. 1400 Ma.
4	Growth of idiomorphic quartz, muscovite, hematite, fluorite, calcite and spherulitic chlorite.	Late-magmatic hydrothermal circulation associated with the Götemar Intrusion.
5	Prehnite, laumonite, calcite, chlorite and fluorite.	Low-temperature burial metamorphism c. 1100 Ma?
6	Illite-dominated mixed-layer clay, calcite, chlorite.	Low-temperature burial metamorphism and mineralisation associated with burial beneath Post-Caledonian sedimentary cover in Sweden.
7	Calcite, Fe-oxyhydroxide, pyrite, clay-minerals? (kaolinite, smectite).	Mineralisation probably associated with Recent/Quaternary groundwater circulation.

2 Results

2.1 CALCITE CL PETROGRAPHY

The fractures contain calcite whose characteristics are largely consistent with those of Calcite generations 2 and 3 as described by Milodowski *et al.* (1998a; Table 2), with evidence for significant fracture rejuvenation, reworking, brecciation and replacement and cementation by later calcite generations. Generation 1 of Milodowski *et al.* (1998a) was not encountered and generation 4 was only tentatively identified in one sample (MPLJ523; 13.95 m). The CL observations have enabled a refinement of Milodowski *et al.'s* (1998a) scheme with the recognition of 4 distinct sub-generations within generation 3 (Table 4; Plate 1; Appendix 1). These generations are primarily recognised on the basis of their CL responses, supported by electron microchemical maps where available (not reported here). Whilst a relatively consistent pattern of zoning can be recognised using CL, it is possible that calcite recognised as a particular generation within one sample is not temporally equivalent to calcite considered to be of the same generation but in a different sample.

Table 4 CL characteristics, distribution and summary fluid inclusion properties for calcite generations 2 and 3.

	Description	Distribution	*(n inclusions with data)*	Salinities	Homogenisation Temperatures
2	orange luminescent, commonly disrupted by later calcite generations	best preserved in upper part of borehole (<255 m)	*(15)*	relatively low, high and very high salinity groups populations represented.	57.5-122°C no monophase
3a	moderate orange-luminescence (Plate 1A), commonly contains well-developed growth and/or sector zoning. Typically clear with only rare fluid inclusions.	throughout	*(26)*	high and very high salinities only	87.5-190°C common monophase
3b	similar in appearance to generation 3a commonly with well-developed growth and sector zoning, but has only dull-orange luminescence.	throughout	*(40)*	relatively low and very high salinity groups	53-195°C common monophase
3c	non- or very-dully luminescent (Plate 1B).	lower part of borehole (>840 m)	*(8)*	predominantly very high salinity	55-95°C no monophase
3d	variably bright orange-luminescence, which may resemble generations 3a or 3b.	throughout	*(12)*	high salinity only	92.5-145°C, no monophase

2.2 FLUID INCLUSION PETROGRAPHY

All the analysed inclusions contain aqueous liquid and vapour, or an aqueous liquid phase only. No hydrocarbon-bearing inclusions were identified during screening using ultraviolet light. Individual inclusions are typically small (of the order of 10 microns diameter), and occur in small clusters and in less-common planes. Given the multiple generations of calcite present and the evidence for reactivation, brecciation, replacement and cementation of earlier generations, "resetting" of earlier-formed inclusions, and formation of new "secondary" inclusions in earlier cements would be expected. The fact that this has occurred is proved in situations where inclusions occurring in close physical proximity have different physical characteristics and/or markedly different salinities (Plate 2). Clusters (or "assemblages") of inclusions were not typically aligned in any particular orientation relative to crystal faces (where recognisable), and in most cases it proved impossible to

definitively identify whether inclusions were of primary (i.e. formed during calcite crystal growth), pseudo-secondary or secondary (i.e. formed at some time after crystal growth, typically healing microfractures) origin. However, it is considered likely that the majority of the analysed inclusions are pseudo-secondary or secondary in origin, and therefore the interpretation of the microthermometric data, particularly in the earlier cement generations which may have "seen" later fluids, has to be treated carefully.

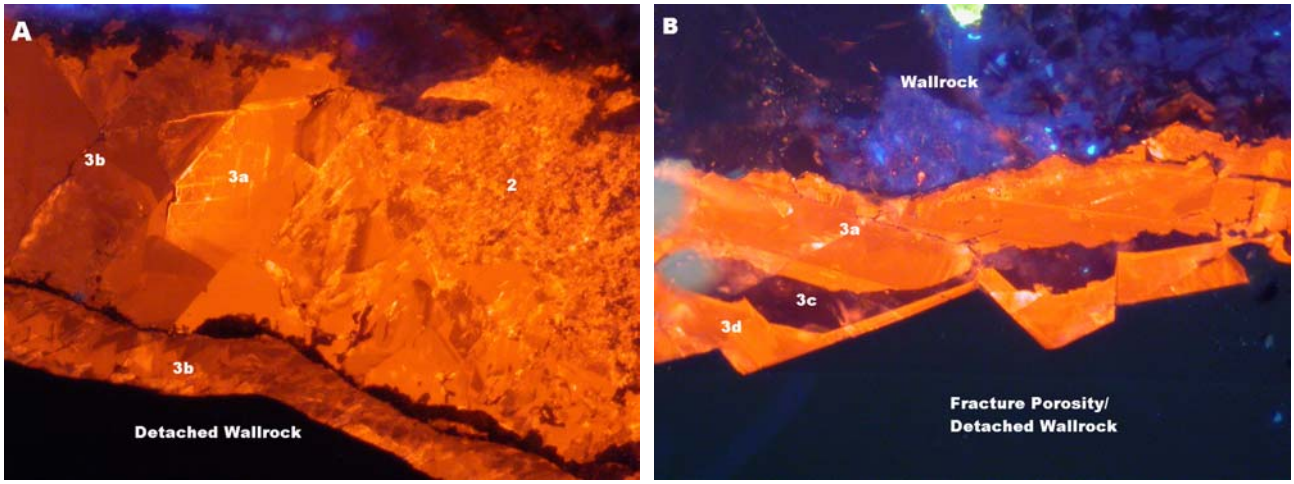

Plate 1 CL images showing the relationships between the different calcite generations.

A) Calcite generation 2 is disrupted, and then overgrown by the moderately orange-luminescent calcite 3a. This is syntaxially overlain by the less strongly orange-luminescent calcite 3b. Fracture re-activation occurred during the precipitation of calcite generation 3b with the development of a thin fracture parallel to the initial fracture which is exclusively filled by calcite of generation 3b. Sample MPLJ549, 223.90 m, field of view 1 mm.

B) Calcite 3a has an anhedral, fracture-filling morphology, and is interpreted to have completely filled the original fracture. This fracture was then reactivated and calcite generations 3c (non-luminescent) and 3d developed with euhedral morphologies as syntaxial overgrowths into the new porosity.

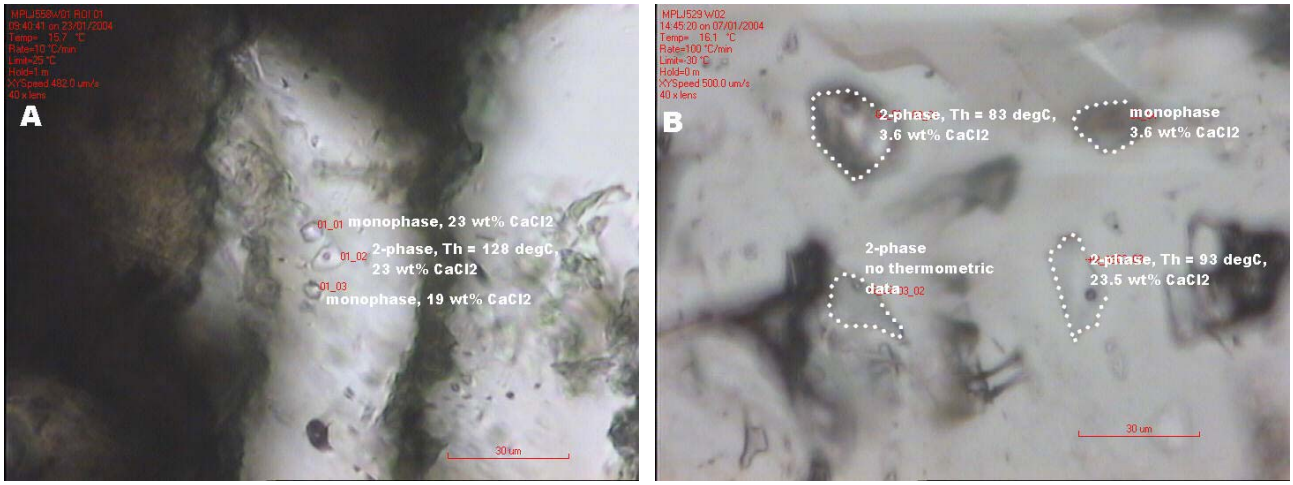

Plate 2 Transmitted light photomicrographs of two assemblages of fluid inclusions within which marked differences in physical characteristics and fluid chemistry are observed.
A) Sample MPLJ558 (939.00 m), inclusion assemblage 1, with a mixture of monophase and 2-phase inclusions and variable salinities (scale bar 30 microns).
B) Sample MPLJ529 (51.30 m), inclusion assemblage 3, with a mixture of monophase and 2-phase inclusions and highly variable salinity (scale bar 30 microns).

2.3 FLUID INCLUSION MICROTHERMOMETRY

Microthermometric data were collected from 100 inclusions in calcite from six samples, with 84 T_{ice}, and 22 T_{fm} determinations (Appendix 2). 33 of the analysed inclusions were monophase at room temperature (no T_h measurement appropriate), and 59 T_h determinations were made on the 2-phase (liquid + vapour) inclusions. It proved impossible to collect any T_{hyd} data.

2.3.1 Homogenisation Temperatures

Aqueous inclusions that are monophase (liquid-only) at room temperature are typically interpreted to indicate that the fluid was trapped at relatively low temperatures although this interpretation is not always valid (Roedder 1984 and Appendix 3). In the 2-phase inclusions, homogenisation temperatures are typically between 50-180°C with a broadly-defined peak between 90-130°C (Figure 1A). No systematic differences in T_h are evident between the samples (or with depth; Figure 2) or between the different calcite cement generations (Figure 1D, Figure 2). However, monophase inclusions appear to be restricted to calcite generations 3a and 3b.

2.3.2 Fluid Composition

Due to the low optical contrast between ice and liquid it proved impossible to determine any T_{fm} for the relatively low salinity inclusions and therefore the nature of the dissolved components in these fluids is unknown.

A number of T_{fm} determinations were possible in the more saline (>8wt% $CaCl_2$ equiv.) inclusions in all the calcite generations. These were all in the region -50 to -60°C, which are probably indicative of mixed NaCl-$CaCl_2$-H_2O brine (with a eutectic, and hence T_{fm} expected at -52°C). In order to estimate NaCl / (NaCl+$CaCl_2$) ratios, and hence derive accurate salinity estimates in this system, determinations of T_{hyd} are required, which proved impossible to observe in these inclusions. However, some of the most saline inclusions (> 21 wt% $CaCl_2$ equiv.) have T_{ice} between -29°C and -25°C, which implies that CaCl / (NaCl + $CaCl_2$) ratios 0.5 or higher, indicating a predominance of $CaCl_2$ over NaCl in these more saline inclusions.

In the absence of paired T_{hyd} and T_{ice} data, and given the inferred high $CaCl_2$ / (NaCl+$CaCl_2$) ratios of some of the most saline inclusions, salinities have been modelled for all inclusions in terms of wt% $CaCl_2$ equivalent, using the freezing point depression data of Oakes *et al.* (1990) for the system $CaCl_2$-H_2O. This will underestimate the salinity of inclusions with lower $CaCl_2$ / (NaCl+$CaCl_2$) ratios at higher salinities (>15 wt% dissolved salt), but is likely to provide reasonable salinity estimates for the lower salinity inclusions, where freezing point suppression is less sensitive to $CaCl_2$ / (NaCl+$CaCl_2$) ratios (Appendix Figure 5).

2.3.3 Salinity

Salinities are highly variable (range 0.8-23.9 wt% $CaCl_2$ equiv; Figure 1), but this range can be broken down into three components:

- a relatively low salinity (brackish) component (range 0-8 wt%, predominantly < 2 wt% $CaCl_2$ equiv). The dissolved species in this component have not been identified (see above).
- a high salinity component (approximately 16-20 wt% $CaCl_2$ equiv.), considered to be a NaCl-$CaCl_2$- H_2O-brine, but of unknown $CaCl_2$ / (NaCl+$CaCl_2$) ratio, and
- a very high salinity component (22-24 wt% $CaCl_2$ equiv.) considered to be a NaCl-$CaCl_2$-H_2O-brine, with $CaCl_2$ / (NaCl+$CaCl_2$) ratio of > 0.5.

In the shallower samples (< 225 m), all three fluid components are observed in approximately sub-equal proportions in the fluid inclusion data, whereas in the deeper samples (> 840 m) the relatively low salinity component appears to be of minor significance (1 inclusion only; Figure 2). There are also some differences in the salinities of the different calcite generations, with generations 2 and 3b

containing both low and high salinity inclusions, generations 3a and 3c appearing to be dominated by high and very high salinity inclusions, and generation 3d containing high salinity inclusions only. No relationships were observed between inclusion salinity and homogenisation temperature.

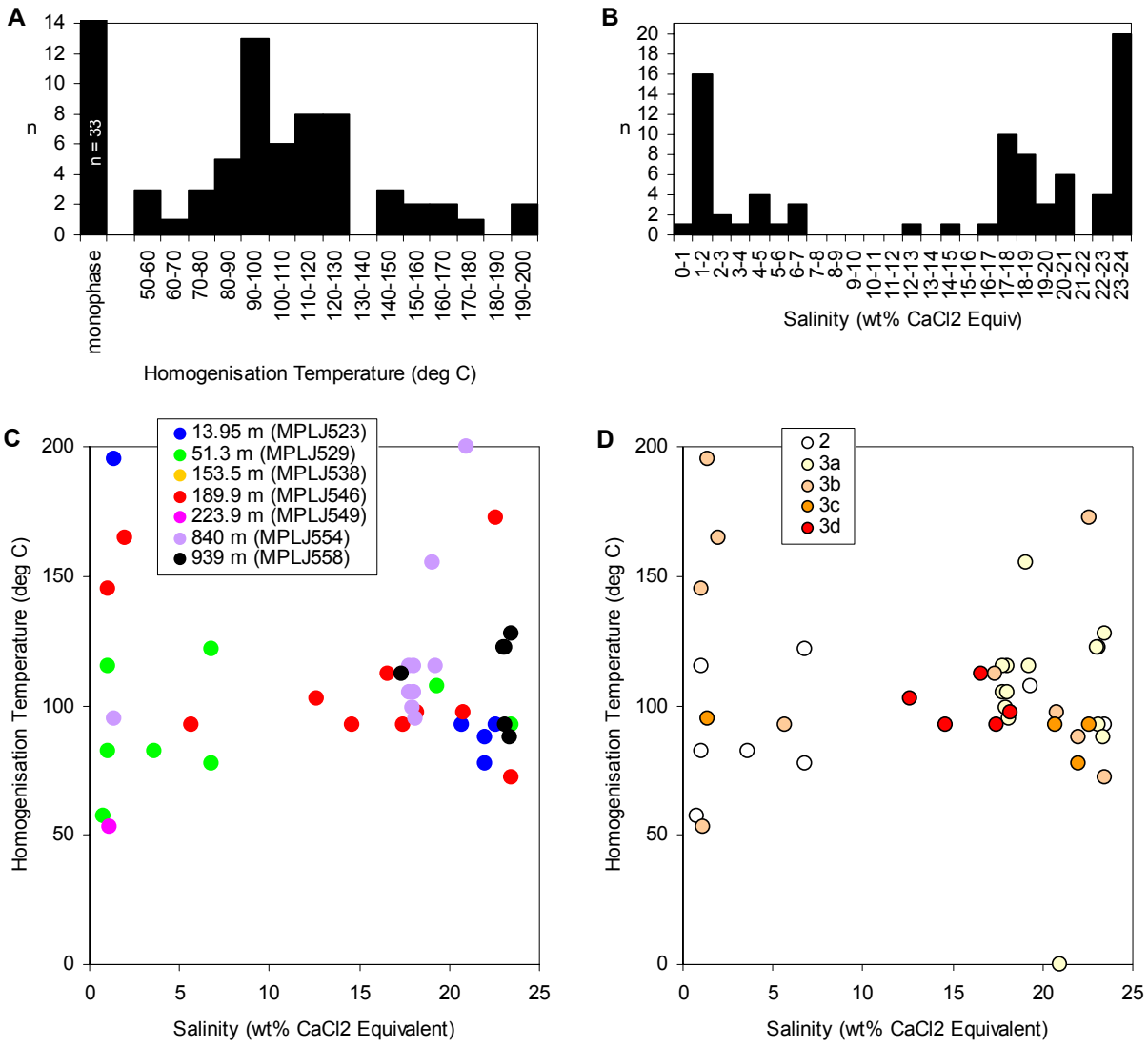

Figure 1 Frequency distributions (A and B) and Cross plots (C and D) showing the fluid inclusion homogenisation temperatures and salinities for all samples. Note plots C and D do not include from monophase inclusions (no T_h data).

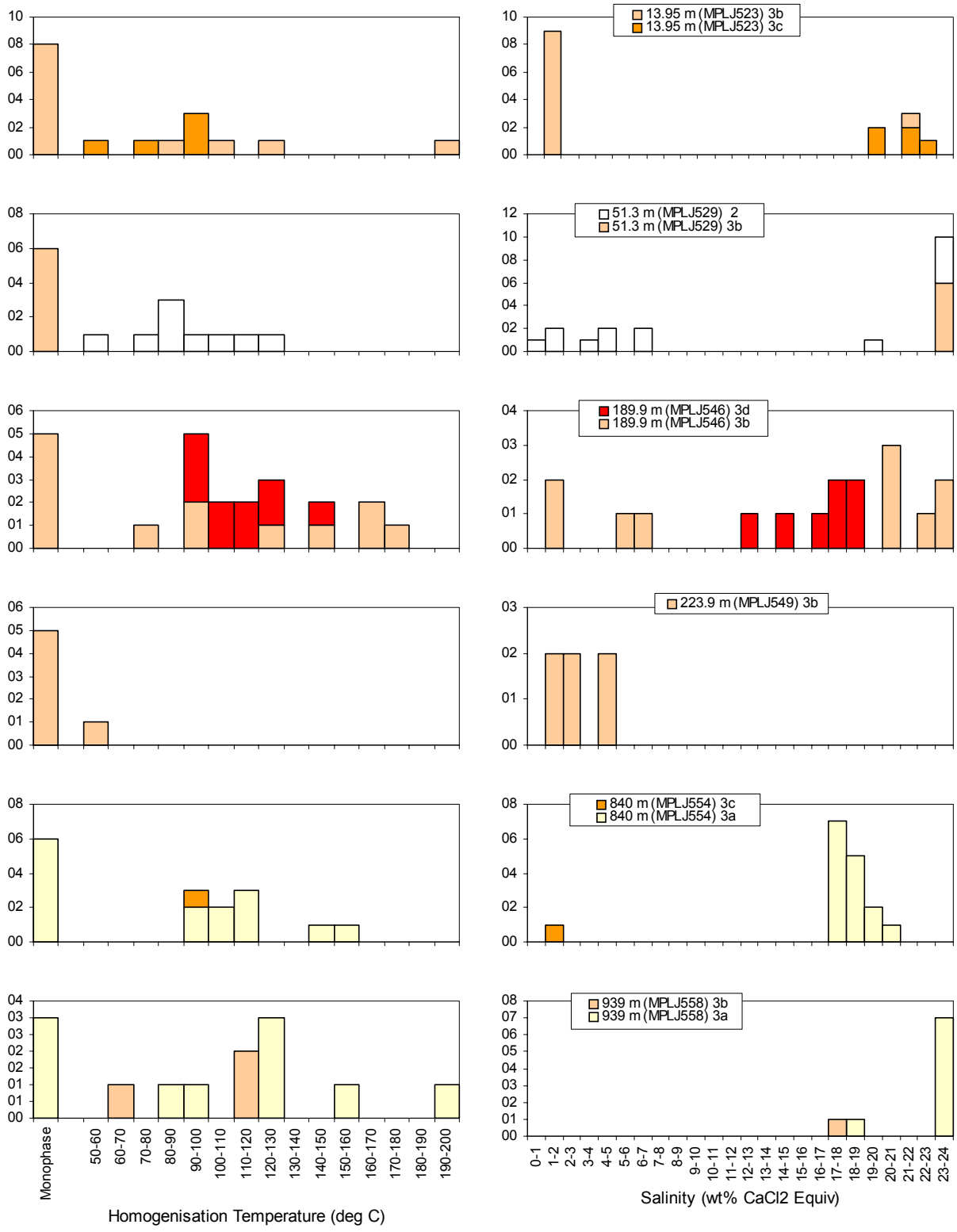

Figure 2 Frequency distributions showing the variations in homogenisation temperature and salinity by sample and calcite generation.

3 Discussion and Conclusions

One of the main limitations of this study has been the difficulty in assessing whether individual inclusions are of primary or secondary origin. This is particularly significant as the older calcite generations will have "seen" the fluids responsible for the precipitation of the younger generations, and hence, in addition to primary inclusions, these generations may also contain secondary inclusions which reflect the composition of younger fluids. This uncertainty is compounded by the possibility that calcite with similar CL characteristics may have developed in different samples at different times. As a result of these uncertainties, the available data are very noisy. However, some useful inferences can be made:

- Homogenisation temperatures are highly variable (53-195°C), and significant proportions of monophase inclusions are also present (33 out of the 100 measured inclusions). Monophase inclusions are usually interpreted to represent trapping relatively low temperatures, which here probably correspond with the lower end of the range of homogenisation temperatures measured for the inclusions containing liquid + vapour. No systematic variations in homogenisation temperature, or in the proportion of monophase vs. liquid + vapour bearing inclusions are observed with depth (note, however, that samples were only available in the intervals <255 m and 840-950 m).
- Salinities are highly variable, and three components are recognised:
  - fresh to brackish fluids (predominantly < 2 wt% $CaCl_2$ equiv), of unknown speciation,
  - a high salinity NaCl-$CaCl_2$-H_2O brine (approximately 16-20 wt% $CaCl_2$ equiv.), of unknown $CaCl_2$ / (NaCl+$CaCl_2$) ratio, and
  - a very high salinity NaCl-$CaCl_2$-H_2O brine (22-24 wt% $CaCl_2$ equiv.) with $CaCl_2$ / (NaCl+$CaCl_2$) ratio of > 0.5.
- Some variations are evident in the character of inclusions from different calcite generations.
  - inclusions in generation 2 contain fluids of relatively low salinity and also of high salinity. This is perhaps not surprising given the extensive alteration, brecciation, replacement and cementation of this generation by later calcite generations. However, it is impossible to distinguish which, if either of the saline or fresh inclusions are of primary origin,
  - generation 3a contains inclusions of high and very high salinity fluids, with no evidence of a fresh water component. This generation is recognised in samples from below 150 m, and is also characterised by relatively high proportions of monophase inclusions.
  - generation 3b contains both relatively fresh and very high salinity fluids, and is characterised by high proportions of monophase inclusions.
  - generation 3c contains predominantly very high salinity inclusions.
  - generation 3d contains high salinity inclusions only.
- High and very high salinity brines appear to occur throughout the borehole, whereas the relatively fresh fluids are largely restricted to the shallower interval (only one inclusion containing fresh fluid was measured from below 840 m). In the adjacent Laxemar-2 borehole (KLX-02), present day groundwaters are low salinity (< 600 mg L^{-1} Cl) down to approximately 1000 m bGL, but below this there is a sharp transition zone with more saline groundwaters (up to 46000 mg L^{-1} Cl; Laasksoharja *et al.* 1999).

  The fact that high salinity fluids are trapped in calcite at relatively shallow depths (<255 m) suggests that either, the transition zone between fresh and saline groundwater was shallower than at the present day during calcite precipitation, or that the calcites are older than previously recognised and related to deep burial or hydrothermal circulation. There are a number of lines

of evidence which support a young age for the calcite, which would suggest a shallower contact between the fresh and saline fluids:

- the relatively low homogenisation temperatures and abundance of monophase inclusions in all calcite generations would suggest relatively cool conditions during calcite growth, and are inconsistent with hydrothermal conditions.
- the restriction of relatively low salinity fluids to calcite generations 2 and 3b may indicate that the low salinity inclusions are, in general, recording older events than the high salinity inclusions.
- Sr-isotope ratios in the youngest calcite generations correspond to the ratios in the present groundwater indicating a possible Quaternary age for these (Tullborg pers. comm.).
- possible grains of grass pollen trapped within the youngest calcite generations in sample MPLJ523 (13.95 m; Milodowski pers. comm.) imply that the youngest calcite must be younger than Palaeogene (<65 Ma; grasses first appeared during the Palaeogene).

Conversely, however, the high Ca:Na ratios inferred for the fluid inclusions are comparable with the Ca:Na ratios of deep brines at the Laxemar site (Na = 8500 ppm; Ca = 19300ppm; total salinity ≈ 7 wt%), and it is therefore possible that the calcite is related to this or similar fluid. On the basis of chlorine isotope data these deep brines are interpreted to have been isolated for more than 1.5 Ma (Tullborg pers. comm.), which would imply that the calcite is of similar age or older.

A possible explanation for this apparent paradox would be that the calcite has been developing over a relatively long time period, and that the youngest generations, from which the Sr-isotope data are derived, have not been captured by the fluid inclusion analysis (either too thinly developed or barren of inclusions).

4 References

BORISENKO, A S. 1977. Study of the salt composition of solutions in gas-liquid inclusions in minerals by the cryogenic method. *Soviet Geology and Geophysics,* Vol. 18(8), 11-19.

LAAKSOHARJA, M, TULLBORG, E-L, WIKBERG, P, WALLIN, B and SMELLIE, J. 1999. Hydrogeochemical conditions and evolution at the Äspö HRL, Sweden. *Applied Geochemistry,* Vol. *14, p.835-859*.

SHEPHERD, T J, RANKIN, A H and ALDERTON, D H M. 1985. A Practical guide to Fluid Inclusion Studies. Blackie, Glasgow and London, ISBN 0-412-00601-4, p.239.

MILODOWSKI, A E, GILLESPIE, M R, PEARCE, J M and METCALFE, R. 1998a. Collaboration with the SKB "EQUIP" programme: petrographic characterisation of calcites from Äspö and Laxemar deep boreholes by scanning electron microscopy, electron microprobe and cathodoluminescence petrography. *British Geological Survey Technical Report,* WG/98/45C.

MILODOWSKI, A E, GILLESPIE, M R, NADEN, J, PEARCE, J M, SHEPHERD, T J, FORTEY, N J and METCALFE, R. 1998b. The petrology and paragenesis of fracture mineralisation in the Sellafield area, west Cumbria. *Proceedings of the Yorkshire Geological Society*, Vol. 52(2), 215-242.

OAKES, C S, BODNAR, R J, and SIMONSON, J M. 1990. The system NaCl-CaCl2-H2O: I. The ice liquidus at 1 atm total pressure. *Geochimica et Cosmochimica Acta,* Vol.54, 603-610.

ROEDDER, E. 1984. Fluid Inclusions. *Mineralogical Society of America, Reviews in Mineralogy,* Vol.12, ISBN 0-939950-16-2.

TULLBORG, E-L. 1995. Mineralogical and chemical data on rocks and fracture mineralisation from Äspö. *SKB Swedish Hard rock Laboratory, Progress report*, 25-90-01.

Appendix 1 Petrographical (CL) Descriptions

This appendix contains brief descriptions of the calcite fracture-fills. Representative CL images are included, with the positions of the analysed fluid inclusion assemblages (FIA), and the different cement generations indicated where appropriate.

Sample MPLJ522 (13.10 m)

This sample contains a < 1mm wide fracture at it's margin and is also cut by a number of 0.1-0.2 mm wide microfractures. These fractures are completely cemented by growth and sector zoned, orange and orange-brown calcite that locally engulf fragments of brecciated wallrock. The calcite is probably of generations Calcite 3a, 3b or 3d.

Sample MPLJ523 (13.95 m)

This sample contains a single fracture (1-2 mm wide), which is filled with multiple generations of calcite (Appendix Plate 3). The earliest has dull orange-luminescence, with some fine-scale zoning (possibly Calcite 3b). On the margin of the fracture where the wall-rock has become detached, this calcite has either been corroded or crystallised with a habit resembling that shown in Plates 11 and 12 of Milodowski *et al*. (1998a; extreme shortening along c-axis). The fracture has been reactivated with precipitation of non-luminescent calcite (3c), which also locally replaces and brecciates the earlier calcite. The last calcite generation (3d) is bright orange-luminescent and occurs on the reactivated margins of the fracture, and along microfractures cutting the earlier calcite generations.

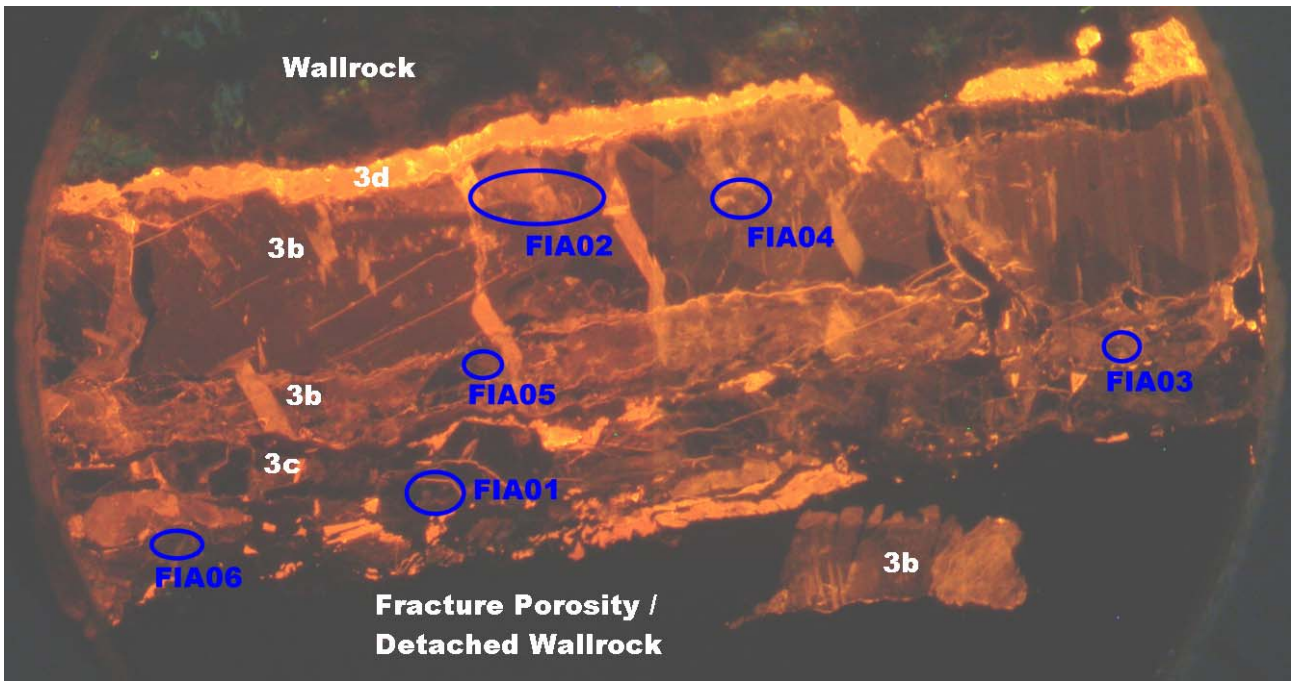

Appendix Plate 3 CL image of analysed region of interest from sample MPLJ523 (13.95 m; field of view = 2.6 mm).

Sample MPLJ527 (37.35 m)

This fracture contains a thin, discontinuous coating of brecciated/disturbed orange luminescent Calcite 2, overlain and replaced by orange luminescent, faintly zoned Calcite 3 (either b or d).

Sample MPLJ529 (51.30 m)

The fractures in this sample are mm-scale and are largely filled by well-developed orange-luminescent, inclusion-rich, un-zoned calcite that engulfs minor blue-luminescent fluorite, and is probably equivalent to Calcite 2 of Milodowski et al. (1998a; Appendix Plate 4A). This is engulfed by two generations of calcite interpreted as being equivalent to Calcite 3 of Milodowski et al. (1998a). The earlier (3b; Appendix Plate 4B) is dully-luminescent and inclusion-poor. This calcite fills relict fracture porosity, occurs lining the margins of new, and also within possibly reactivated older fractures. In turn, this is fractured and re-cemented, and overgrown by a later generation (termed 3d) of orange-luminescent, locally zoned, inclusion-poor calcite.

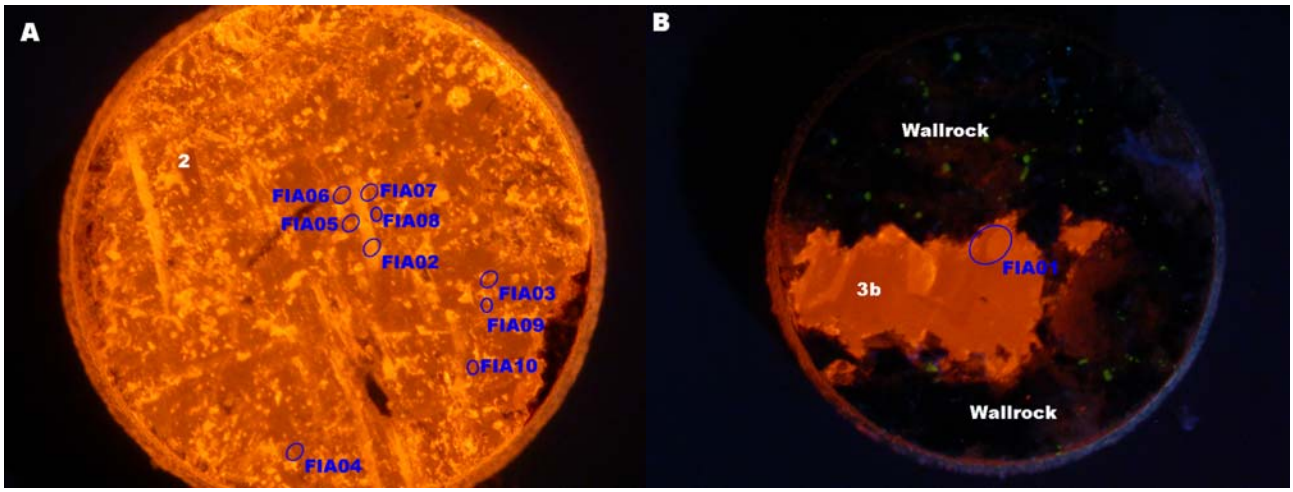

Appendix Plate 4 CL images of analysed regions of interest from sample MPLJ529 (51.30 m). A) region 2, Calcite 2 (field of view = 2.0 mm). B) region 1, Calcite 3b (field of view = 2.0 mm).

Sample MPLJ532 (60.00 m)

This sample contains a epidote-filled vein (c. 3 mm wide) which has been reactivated and cemented by 3 distinct calcite generations. The earliest (Calcite 2) is orange luminescent, and is commonly disrupted, locally brecciated, by the later generations. This is overlain by a euhedral coating of non- and dully-luminescent euhedral calcite (Calcites 3b and/or 3c) at the fracture margin. The euhedral nature of this generation suggests growth into open space, and hence implies fracture rejuvenation and dilation. This calcite is engulfed by orange luminescent, euhedral calcite (Calcite 3d).

Sample MPLJ538 (153.50 m)

The fracture in this sample is coated by isolated, individual crystals of orange and orange-brown luminescent calcite (probably generation 3a), which are strongly growth and sector zoned. No workable inclusions could be found within this calcite.

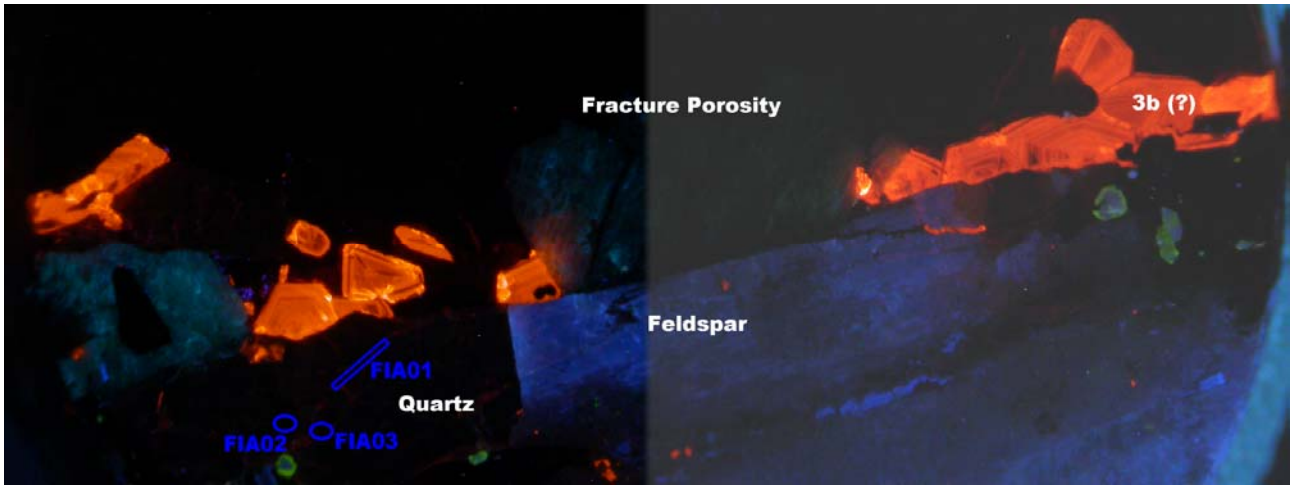

Appendix Plate 5 CL image of analysed region of interest from sample MPLJ538 (153.50 m; field of view = 3.4 mm).

Sample MPLJ546 (189.50 m)

The earliest, orange-luminescent calcite fill in this fracture (Calcite 2) is brecciated, replaced and overgrown by 3 generations of variably non- to orange-luminescent calcite (Calcite 3a, 3b and 3d; Appendix Plate 6). The youngest of these (Calcite 3d) locally forms euhedral outgrowths.

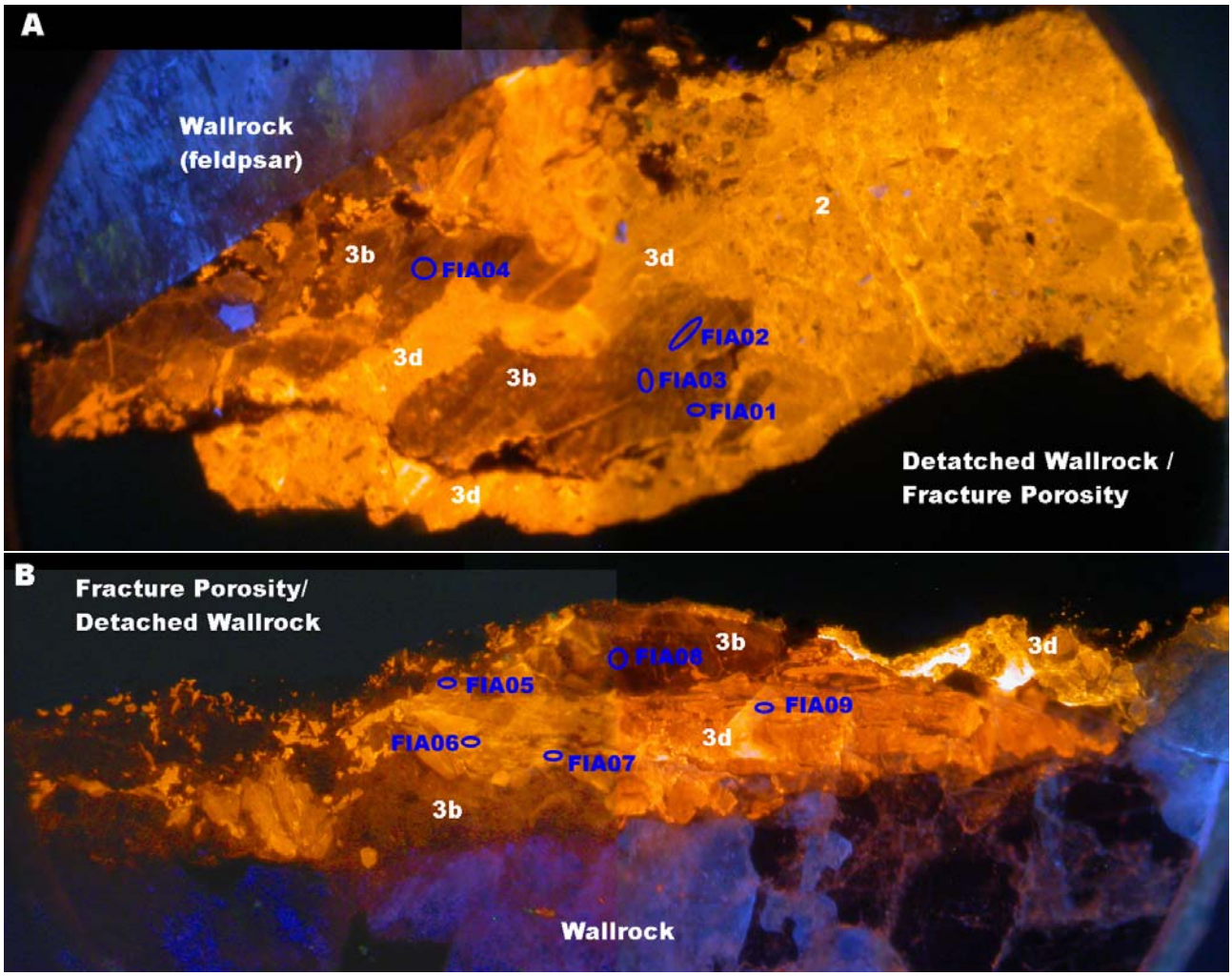

Appendix Plate 6 CL images of analysed regions of interest from sample MPLJ546 (189.50m). A) Region 1, (field of view = 3.2 mm). B) Region 2 (field of view = 3.2 mm).

Sample MPLJ549 (223.90 m)

This fracture contains disrupted, orange-luminescent calcite (2; Appendix Plate 7), which has been progressively overgrown by clear orange luminescent calcite (3a) and dull orange-brown luminescent, zoned calcite (3b). Calcite 3a is constrained to within the fracture aperture that would have been present during precipitation of Calcite 2. However, prior to the formation Calcite 3b, the fracture was dilated resulting the formation of calcite 3b overgrowths on earlier the generations in the new fracture porosity.

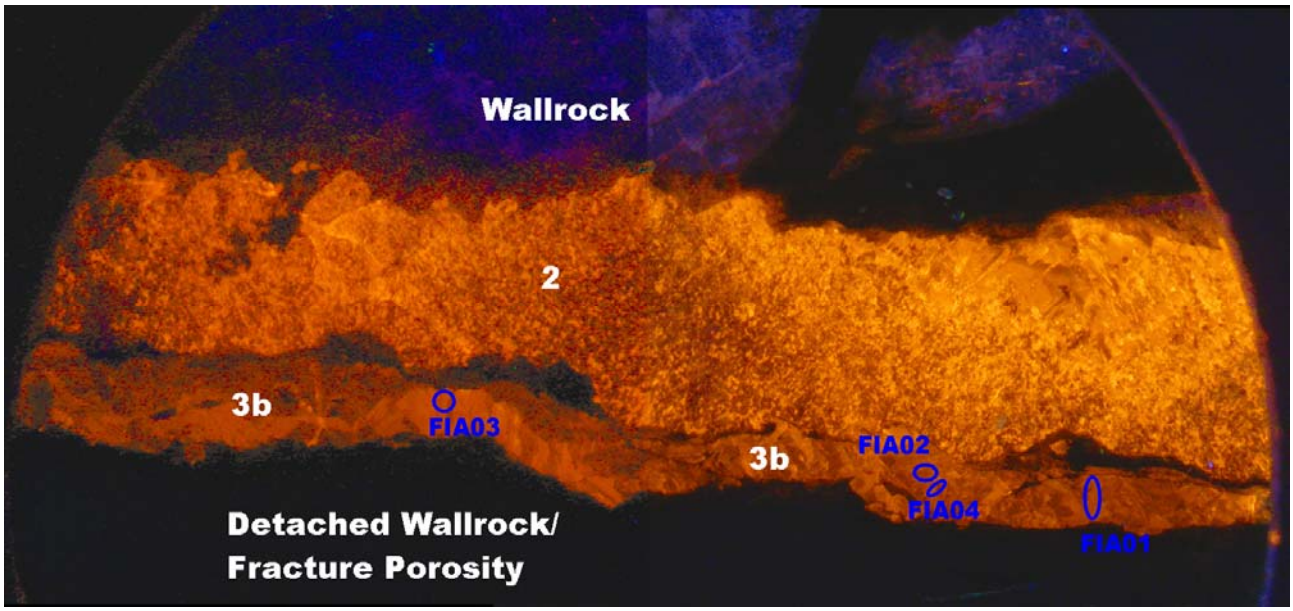

Appendix Plate 7 CL image of analysed region of interest from sample MPLJ549 (223.90 m; field of view = 3.2 mm).

Sample MPLJ551 (255.00 m)

This fracture contains a poorly-developed coating of orange luminescent calcite, commonly with a lath-shaped morphology suggesting pseudomorphism of an earlier fracture-filling phase. The generation(s) into which this calcite falls is uncertain.

Sample MPLJ554 (840.00 m)

The fracture in this sample displays well-developed growth zoning with three distinct calcite generations present. The earliest is orange-brown luminescent (3a; Appendix Plate 8) with well-developed internal zonation. This is overlain by euhedral overgrowths of non-luminescent calcite (3c). The youngest generation (3d) is orange-brown luminescent and forms euhedral overgrowths on the earlier generations.

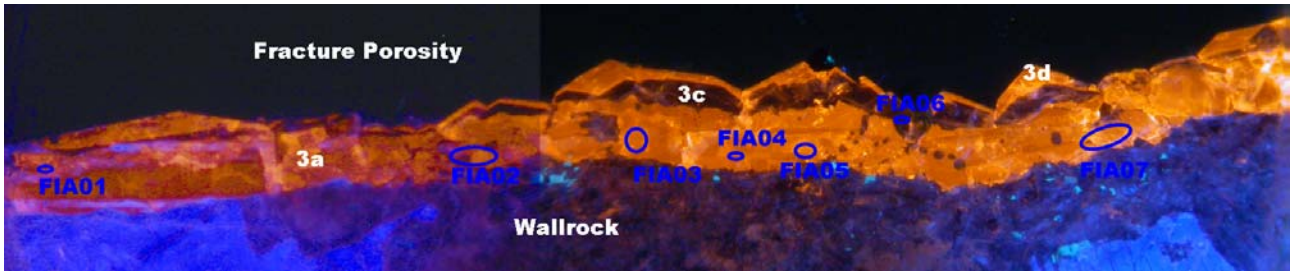

Appendix Plate 8 CL image of analysed region of interest from sample MPLJ554 (840.00 m; field of view = 3.3 mm).

Sample MPLJ557 (936.80 m)

The sample contains a discontinuous fracture filled with orange luminescent calcite (2 or 3a). This calcite is overgrown by a generation of non-luminescent, euhedral calcite (3c) followed by an orange-brown dully-luminescent generation (3d).

Sample MPLJ558 (939.00 m)

The bulk of this fracture is filled with moderately orange-brown luminescent calcite with well-developed intra-sector zoning, and less well developed growth zoning (Calcite 3b). The margins of the fracture contain disrupted, inclusion-rich orange luminescent calcite (2 or 3a) which may have been replaced by calcite 3b. The fracture has been reactivated with opening of the fracture aperture on one side only. Along this opening orange luminescent calcite (3a) has precipitated. Further dilation then occurred before the development of two generations of euhedral calcite (3c and 3d) in the resulting porosity. As in sample MPLJ557, calcite 3c is non-luminescent, and calcite 3d is dully orange-brown luminescent.

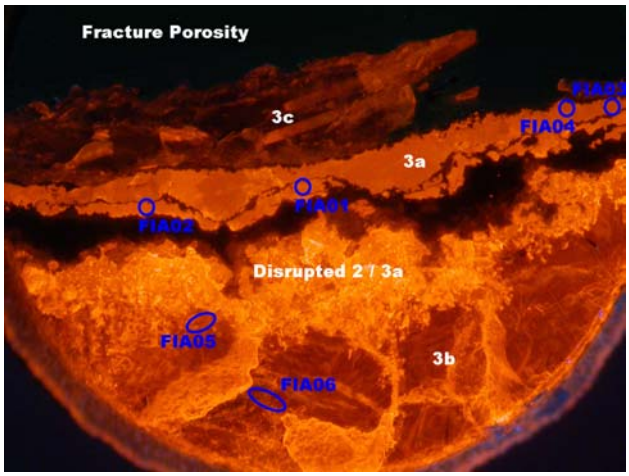

Appendix Plate 9 CL image of analysed region of interest from sample MPLJ558 (939.00 m; field of view = 2.0 mm).

Sample MPLJ559 (945.34 m)

This fracture contains the same paragenetic sequence as that described above for sample MPLJ558.

Appendix 2 Fluid Inclusion Microthermometric Data

Appendix Table 5 Listing of fluid inclusion microthermometric data for fracture-filling calcites from KLX-10 (page 1 of 2).

Sample	Depth (m)	Inclusion ID	Phases present at room temperature	Size (microns)	Calcite Generation	Degree of Fill (%)	Th (error)	Tfm (error)	Tice (error)	Salinity (wt% $CaCl_2$ Equiv.)	MINIMUM estimate CaCl2(NaCl+CaCl2)	COMMENT
MPLJ523	13.95	01_01	aq L+V	5	3c	95	55.0 +/- 5.0					
MPLJ523	13.95	01_02	aq L+V	5	3c	95			-19.0 +/- 0.2	20.2		
MPLJ523	13.95	01_04	aq L+V	5	3c	95	92.5 +/- 2.5		-20.3 +/- 0.1	20.7		
MPLJ523	13.95	01_05	aq L+V	10	3c				-27.5 +/- 0.5	23.4	0.62	
MPLJ523	13.95	02_01	aq L+V	40	3b	95	102.5 +/- 2.5					
MPLJ523	13.95	02_02	aq L-only	15	3b	100			-0.7 +/- 0.1	1.4		
MPLJ523	13.95	02_03	aq L-only	15	3b	100			-0.6 +/- 0.1	1.2		
MPLJ523	13.95	02_05	aq L-only	10	3b	100			-0.5 +/- 0.1	1.0		
MPLJ523	13.95	02_06	aq L-only	10	3b	100			-0.5 +/- 0.1	1.0		
MPLJ523	13.95	03_01	aq L+V	5	3b	90	122.5 +/- 2.5					leaked after Th.
MPLJ523	13.95	04_01	aq L+V	20	3b	80	195.0 +/- 5.0		-0.7 +/- 0.1	1.4		
MPLJ523	13.95	04_02	aq L-only	15	3b	100			-0.6 +/- 0.1	1.2		
MPLJ523	13.95	04_04	aq L-only	15	3b	100			-0.5 +/- 0.1	1.0		
MPLJ523	13.95	04_05	aq L-only	15	3b	100			-0.5 +/- 0.1	1.0		
MPLJ523	13.95	04_06	aq L-only	15	3b	100			-0.5 +/- 0.1	1.0		
MPLJ523	13.95	05_01	aq L+V	5	3b	95	87.5 +/- 2.5		-23.5 +/- 0.5	22.0	0.49	
MPLJ523	13.95	06_01	aq L+V	15	3c	95	77.5 +/- 2.5	-55.0 +/- 5.0	-23.5 +/- 0.5	22.0	0.49	
MPLJ523	13.95	06_03	aq L+V	5	3c	95	92.5 +/- 2.5		-25.0 +/- 1.0	22.6	0.54	
MPLJ523	13.95	06_04	aq L+V	5	3c	95	92.5 +/- 2.5					
MPLJ529	51.30	01_01	aq L-only	4	3b	100		-52.5 +/- 2.5	-29.0 +/- 1.0	23.9	0.67	
MPLJ529	51.30	01_02	aq L-only	2	3b	100			-29.0 +/- 1.0	23.9	0.67	
MPLJ529	51.30	01_03	aq L-only	5	3b	100		-52.5 +/- 2.5	-28.4 +/- 0.2	23.7	0.65	
MPLJ529	51.30	01_04	aq L-only	10	3b	100		-55.0 +/- 5.0	-28.4 +/- 0.2	23.7	0.65	
MPLJ529	51.30	01_05	aq L-only	10	3b	100			-28.4 +/- 0.2	23.7	0.65	
MPLJ529	51.30	01_06	aq L-only	5	3b	100			-28.4 +/- 0.2	23.7	0.65	
MPLJ529	51.30	02_01	aq L+V	30	2	99	82.5 +/- 2.5					leaked after Th.
MPLJ529	51.30	02_02	aq L+V	15	2	95	122.0 +/- 2.0		-3.8 +/- 0.2	6.7		
MPLJ529	51.30	02_03	aq L+V	20	2	95	77.5 +/- 2.5		-3.8 +/- 0.2	6.7		
MPLJ529	51.30	03_01	aq L+V	25	2	95	82.5 +/- 2.5		-1.9 +/- 0.1	3.6		
MPLJ529	51.30	03_03	aq L+V	25	2	99	92.5 +/- 2.5	-58.0 +/- 2.0	-27.7 +/- 0.1	23.5	0.63	
MPLJ529	51.30	03_04	aq L+V	15	2	99			-2.5 +/- 0.2	4.7		
MPLJ529	51.30	04_01	aq L+V	30	2	99	57.5 +/- 2.5		-0.4 +/- 0.2	0.8		
MPLJ529	51.30	05_01	aq L+V	20	2	95	107.5 +/- 2.5		-17.4 +/- 0.2	19.4		
MPLJ529	51.30	06_01	aq L+V	30	2	95	82.5 +/- 2.5		-0.5 +/- 0.1	1.0		
MPLJ529	51.30	07_01	aq L+V	25	2	95	115.0 +/- 5.0		-0.5 +/- 0.1	1.0		
MPLJ529	51.30	08_01	aq L+V	15	2	95			-2.3 +/- 0.1	4.3		
MPLJ529	51.30	09_01	aq L+V	8	2				-27.1 +/- 0.1	23.3	0.61	
MPLJ529	51.30	09_02	aq L+V	8	2				-27.1 +/- 0.1	23.3	0.61	
MPLJ529	51.30	10_01	aq L+V	30	2				-27.1 +/- 0.1	23.3	0.61	

Appendix Table 5 Listing of fluid inclusion microthermometric data for fracture-filling calcites from KLX-10 (page 2 of 2).

Sample	Depth (m)	Inclusion ID	Phases present at room temperature	Size (microns)	Calcite Generation	Degree of Fill (%)	Th (error)	Tfm (error)	Tice (error)	Salinity (wt% $CaCl_2$ Equiv.)	MINIMUM estimate CaCl2(NaCl+CaCl2)	COMMENT
MPLJ546	189.90	01_01	aq L+V	8	3b	90	92.5 +/- 2.5		-3.1 +/- 0.1	5.6		
MPLJ546	189.90	02_01	aq L+V	15	3b	90	165.0 +/- 5.0					leaked after Th.
MPLJ546	189.90	02_02	aq L+V	10	3b	90	125.0 +/- 5.0					leaked after Th.
MPLJ546	189.90	02_03	aq L+V	5	3b	90	165.0 +/- 5.0		-1.0 +/- 0.1	2.0		
MPLJ546	189.90	03_01	aq L-only	7	3b	100			-3.4 +/- 0.2	6.1		indistinct Tice
MPLJ546	189.90	04_01	aq L+V	8	3b	90	145.0 +/- 5.0		-0.5 +/- 0.1	1.0		
MPLJ546	189.90	04_02	aq L+V	10	3b	90	72.5 +/- 2.5		-27.5 +/- 0.5	23.4	0.62	
MPLJ546	189.90	05_01	aq L+V	7	3b	90	97.5 +/- 2.5		-20.5 +/- 0.1	20.8		
MPLJ546	189.90	05_02	aq L-only	7	3b	100		-56.0 +/- 2.0	-20.5 +/- 0.1	20.8		
MPLJ546	189.90	05_03	aq L-only	7	3b	100		-56.0 +/- 2.0	-20.5 +/- 0.1	20.8		
MPLJ546	189.90	06_01	aq L+V	15	3d	90	92.5 +/- 2.5	-55.0 +/- 5.0	-10.4 +/- 0.2	14.6		some leakage during heating run
MPLJ546	189.90	06_02	aq L+V	10	3d	90	102.5 +/- 2.5	-55.0 +/- 5.0	-8.4 +/- 0.2	12.6		
MPLJ546	189.90	06_03	aq L+V	7	3d	90	145.0 +/- 5.0					
MPLJ546	189.90	07_01	aq L+V	15	3d	95	97.5 +/- 2.5		-15.3 +/- 0.1	18.2		some leakage during heating run
MPLJ546	189.90	07_02	aq L+V	10	3d	95	92.5 +/- 2.5		-14.1 +/- 0.1	17.4		some leakage during heating run
MPLJ546	189.90	07_03	aq L+V	10	3d	95	107.5 +/- 2.5					
MPLJ546	189.90	07_04	aq L+V	7	3d	95	125.0 +/- 5.0					
MPLJ546	189.90	07_05	aq L+V	7	3d	95	112.5 +/- 2.5		-12.9 +/- 0.1	16.6		
MPLJ546	189.90	07_06	aq L+V	7	3d	95			-15.1 +/- 0.1	18.1		
MPLJ546	189.90	07_07	aq L+V	7	3d	95			-13.7 +/- 0.1	17.2		
MPLJ546	189.90	08_01	aq L-only	10	3b	100		-65.0 +/- 5.0				
MPLJ546	189.90	08_02	aq L+V	7	3b	95	172.5 +/- 2.5		-25.0 +/- 0.2	22.6	0.54	
MPLJ546	189.90	08_03	aq L-only	10	3b	100		-65.0 +/- 5.0	-27.3 +/- 0.1	23.4	0.61	
MPLJ546	189.90	09_02	aq L+V	10	3d	90	117.5 +/- 2.5					leaked after Th.
MPLJ546	189.90	09_03	aq L+V	5	3d	90	125.0 +/- 5.0					leaked after Th.
MPLJ549	223.90	01_01	aq L+V	20	3b	99	53.0 +/- 3.0		-0.6 +/- 0.1	1.1		
MPLJ549	223.90	01_03	aq L-only	10	3b	100			-0.7 +/- 0.1	1.4		
MPLJ549	223.90	02_01	aq L-only	7	3b	100			-1.1 +/- 0.1	2.2		
MPLJ549	223.90	03_01	aq L-only	5	3b	100			-2.5 +/- 0.1	4.7		
MPLJ549	223.90	03_02	aq L-only	5	3b	100			-2.5 +/- 0.1	4.7		
MPLJ549	223.90	04_01	aq L-only	10	3b	100			-1.2 +/- 0.2	2.3		
MPLJ554	840.00	01_01	aq L+V	8	3a	95	95.0 +/- 1.0	-67.0 +/- 3.0	-15.2 +/- 0.2	18.1		
MPLJ554	840.00	01_02	aq L-only	4	3a	100			-15.2 +/- 0.2	18.1		
MPLJ554	840.00	01_03	aq L+V	6	3a	95	99.0 +/- 1.0	-60.0 +/- 5.0	-14.9 +/- 0.1	17.9		
MPLJ554	840.00	02_01	aq L+V	5	3a	99	115.0 +/- 5.0		-15.1 +/- 0.1	18.1		
MPLJ554	840.00	02_04	aq L-only	4	3a	100			-14.7 +/- 0.1	17.8		
MPLJ554	840.00	02_05	aq L-only	4	3a	100			-14.9 +/- 0.1	17.9		
MPLJ554	840.00	02_06	aq L-only	4	3a	100			-15.4 +/- 0.2	18.2		
MPLJ554	840.00	03_01	aq L+V	15	3a	50	>200	-55.0 +/- 5.0	-20.8 +/- 0.2	20.9	0.38	indistinct Tice
MPLJ554	840.00	03_02	aq L+V	8	3a	90	155.0 +/- 5.0	-55.0 +/- 5.0	-16.8 +/- 0.2	19.0		
MPLJ554	840.00	03_03	aq L-only	7	3a	100		-55.0 +/- 5.0	-14.7 +/- 0.1	17.8		
MPLJ554	840.00	03_03	aq L-only	15	3a	100		-55.0 +/- 5.0	-14.9 +/- 0.1	17.9		necked inclusion.
MPLJ554	840.00	04_01	aq L+V	20	3a	90	142.5 +/- 2.5					leaked during heating run (after Th)
MPLJ554	840.00	04_02	aq L+V	10	3a	90	115.0 +/- 5.0		-17.1 +/- 0.2	19.2		
MPLJ554	840.00	05_01	aq L+V	8	3a	95	115.0 +/- 5.0		-14.7 +/- 0.1	17.8		
MPLJ554	840.00	05_02	aq L+V	2	3a	95	105.0 +/- 5.0		-14.7 +/- 0.1	17.8		
MPLJ554	840.00	06_01	aq L+V	3	3c	95	95.0 +/- 5.0		-0.7 +/- 0.1	1.4		metastable Tice
MPLJ554	840.00	07_01	aq L+V	12	3a	99	105.0 +/- 5.0	-57.0 +/- 3.0	-15.0 +/- 0.2	18.0		
MPLJ558	939.00	01_01	aq L-only	8	3a	100		-57.5 +/- 2.5	-26.8 +/- 0.1	23.2	0.60	
MPLJ558	939.00	01_02	aq L+V	10	3a	95	127.5 +/- 2.5	-57.5 +/- 2.5	-27.5 +/- 0.1	23.4	0.62	
MPLJ558	939.00	01_03	aq L-only	5	3a	100			-16.6 +/- 0.2	18.9		
MPLJ558	939.00	02_01	aq L+V	10	3a	99	92.5 +/- 2.5	-60.0 +/- 2.5	-26.5 +/- 0.1	23.1	0.59	
MPLJ558	939.00	03_02	aq L-only	4	3a	100			-26.5 +/- 0.1	23.1	0.59	
MPLJ558	939.00	03_04	aq L+V	7	3a	99	87.5 +/- 2.5		-27.3 +/- 0.1	23.4	0.61	
MPLJ558	939.00	04_01	aq L+V	3	3a	95	122.5 +/- 2.5		-26.5 +/- 0.1	23.1	0.59	
MPLJ558	939.00	04_02	aq L+V	3	3a	95	122.5 +/- 2.5		-26.3 +/- 0.1	23.0	0.58	
MPLJ558	939.00	04_03	aq L+V	4	3a	95	190.0 +/- 5.0					
MPLJ558	939.00	04_04	aq L+V	5	3a	95	157.5 +/- 2.5					
MPLJ558	939.00	05_01	aq L+V	10	3b	95	112.5 +/- 2.5					
MPLJ558	939.00	05_02	aq L+V	10	3b	95	65.0 +/- 5.0					leaked after Th.
MPLJ558	939.00	06_01	aq L+V	20	3b	90	112.5 +/- 2.5	-55.0 +/- 5.0	-14.0 +/- 2.0	17.4		indistinct Tice, leaked after first freezing run.

Appendix 3 Methodology

FLUID INCLUSION ANALYSIS

Fluid Inclusion Wafer Preparation

Blue-dye resin impregnated, doubly-polished fluid inclusion wafers (40-50 μm thick) were prepared in the BGS thin-sectioning facility using standard techniques (Shepherd *et al.* 1985), and bonded to a glass cover slip which increases sample competency during subsequent handling.

Preliminary Screening

Transmitted light microscopy was used to identify "regions of interest" on each fluid inclusion wafer which contain fluid inclusions of sufficient size and abundance for microthermometric analysis. These regions of interest were then extracted from the wafer as circular disks of approximately 2-7 mm diameter using a micro-drill attached to an optical microscope. These disks were then transferred to the heating-freezing stage for analysis.

Microthermometry

Fluid inclusion microthermometry was conducted using a Linkam MDS600 heating-freezing stage, attached to a Leitz Ortholux II microscope, controlled by Linksys software and a Linkam TP93 programmer. A temperature calibration check was performed using synthetic fluid inclusion standards. The controller was reprogrammed if the measured temperatures differed from the known values by more than ±0.1°C.

For the determination of all phase changes a "cycling" protocol, compatible with the general methodology for the study of fluid inclusions in diagenetic cements outlined by Goldstein & Reynolds (1995), was applied. This protocol takes advantage of the fact that nearly all phase changes exhibit some degree of metastability on cooling. The temperature of the end point of a phase change was approached incrementally, followed by rapid cooling of the inclusion. If the end-point of the phase change has not been passed, then the "disappearing" phase (e.g. vapour bubble, ice crystal) typically returns gradually. If the end point has been passed, the "disappearing" phase typically only returns after cooling by several 10's of °C. The errors in determination of phase changes are thus controlled by the temperature increment used during the approach to the end point of the phase change being measured. Errors are typically:

- homogenisation temperatures (T_h): between ±2.5 - ±5°C,
- final ice melting (T_{ice}): between ±0.2 - ±0.1°C,
- for first ice melting (T_{fm}): between ±5°C,

No pressure corrections have been applied to the homogenisation temperatures. The relatively large error on the T_{fm} data is due to the indistinct nature of first melting observations, rather than any instrumental limitation.

For two-phase (aqueous liquid + vapour) inclusions, T_h was determined on "heating runs" prior to the determination T_{fm} and T_{ice}. on "freezing runs". This strategy prevents homogenisation temperatures being artificially elevated due to inclusion "stretching" during freezing. Although attempts were made to measure and salt-hydrate melting (T_{hyd}) no such data could be obtained.

Salinity Determination for Monophase Inclusions

A significant number of monophase (contain liquid only at room temperature) inclusions were also analysed. The ability of an inclusion to nucleate a vapour phase on cooling is related to the interplay between shrinkage of the fluid on cooling (increases internal tension which tends to form a vapour bubble) and the surface tension of the liquid phase (which tends to collapse the bubble; Roedder 1984). In inclusions where the stable vapour phase is sufficiently small in proportion to the size of the entire inclusion and surface tension is able to overcome the internal tension, fluids may become "stretched". This may occur in small inclusions trapped at high temperature, or in larger inclusions trapped at lower temperature. Therefore, although a large inclusion trapped at high temperature would be anticipated to nucleate a vapour phase on cooling to room temperature (and conversely a large monophase inclusion at room temperature may indicate relatively low trapping temperature conditions), the absence of a vapour phase in an inclusion can not be taken to definitively indicate trapping at low temperature.

In addition, T_{ice} data are only reliable for the calculation of bulk salinities if measured when a vapour phase is present in the inclusion. Therefore, in order to derive ice melting, and hence derive salinities for monophase inclusions, the following strategies were applied:

1. Heating runs to determine T_h of 2-phase inclusions within a sample commonly required heating of the sample to approximately 200°C. This sometimes caused sufficient deformation and/or leakage of monophase inclusions that when the sample was cooled to room temperature a vapour phase nucleated, enabling determination of ice melting temperatures. Freezing runs were then undertaken on any, originally monophase, inclusions that had nucleated a vapour phase due to this process prior to attempting any other strategies.
2. In the event that strategy 1 failed to generate a vapour phase in the monophase inclusions of interest, an attempt was made to deform or stretch the inclusion walls by freezing the inclusion rapidly to -100°C followed by more gradual warming to room temperature. Freezing runs were then conducted on those inclusions within which a vapour phase had been induced. However, even following repeated freeze-thaw cycles, this strategy was unable to consistently generate a vapour phase.

   In both of the above strategies, following the nucleation of a vapour phase in a stretched (or leaked) inclusion, it was commonly observed that the vapour phase was lost on freezing and failed to re-nucleate before final ice melting.
3. The final strategy exploits the fact that in minerals such as calcite, inclusions heated to temperatures above their homogenisation temperature commonly undergo deformation and stretching, which may be accompanied by leakage of fluid. In inclusions that do not contain daughter minerals at the point of leakage it is probably safe to assume that any fluid lost will be of the same composition as the bulk inclusion (i.e. the loss is isochemical), and consequently that salinity data derived from ice melting in an inclusions leaked in this manner should reflect the original composition of the inclusion.

   The procedure adopted a step wise strategy with heating in increments of 50°C, followed by cooling to <5°C and inspection of the target inclusions for the development of a vapour phase. Freezing runs were then performed on any inclusions within which vapour phases had been induced, prior to running the next heating increment. The maximum temperature used for this strategy was 300°C, during which total leakage/decrepitation of 2-phase inclusions was commonly observed. Because this strategy carries a risk of causing decrepitation of inclusions within the sample, this was only employed if strategies 1 and 2 failed to yield sufficient numbers of inclusions with vapour phases suitable for T_{ice} determination.

GLOSSARY OF FLUID INCLUSION MICROTHERMOMETRY AND TERMINOLOGY

T_{fm} (Temperature of First Melting) This is the temperature at which the first liquid is observed in the fluid inclusion after freezing and is an estimate of the eutectic temperature. The eutectic temperature is dependant upon the number and type of components in the fluid system, but is independent of salinity. The eutectic of the system NaCl-H_2O is at -21.2°C, and that of the system NaCl-H_2O-$CaCl_2$ is at -52°C. Eutectic temperatures are difficult to determine in low salinity fluids due to the small refractive index contrast between ice and liquid, and consequently observed temperatures of first melting are commonly too high.

T_{ice} (Temperature of Final Ice Melting) Where ice is the only low-temperature solid phase observed to melt, ice melting can be used to estimate salinity. Where additional phases are present after first-melting (e.g. salts and salt-hydrates) then final ice melting alone cannot be used to estimate salinity and other parameters related to salt dissolution or hydrate melting are required.

T_{hyd} (Temperature of Salt-Hydrate Melting) This is the temperature at which specific salt-hydrate phases (e.g. hydrohalite) melt/dissolve. Where the fluids are simple two-component salt-water systems, salt-hydrate-melting can be used to directly estimate salinity. However, for more complex systems (e.g. NaCl-H_2O-$CaCl_2$) then other phase changes, such as ice melting are required to determine the bulk salinity and weight percentage of salts in solution.

T_{halite} (Temperature of Halite Melting) At high salinities, fluid inclusions may contain daughter minerals such as halite. The temperature at which these daughter minerals melt/dissolve can be used to estimate the salinity of the fluid.

T_h (Temperature of Homogenisation) This is the temperature at which the fluid inclusion becomes monophase, and for general purposes corresponds to the disappearance of the vapour phase. If the inclusion has undergone no post-trapping modifications, T_h provides an estimate of the minimum temperature of trapping.

wt% salt equivalent (wt% salt equiv.) This is an estimation of the total amount of salts dissolved in an inclusion and is based on the assumption that the salts are either NaCl or $CaCl_2$, or, where paired hydrohalite and ice-melting data are available, the combined amount of NaCl and $CaCl_2$.

NaCl / (NaCl + $CaCl_2$) wt ratio This is the weight proportion of NaCl and $CaCl_2$ in a fluid inclusion estimated from paired hydrohalite and ice-melting data.

FIA (*Fluid Inclusion Assemblage*) This term denotes a group of inclusions with similar optical properties occurring within the same locale (e.g. a single plane of primary inclusions at a grain-overgrowth boundary). The inference is that the inclusions within an assemblage are approximately contemporaneous and/or otherwise related to each other.

Abbreviations used on data sheets (Appendix 2):

Inclusion Type:	*aq (Aqueous)*	The inclusion contains an aqueous fluid (brine or pure water).
	L + V	The inclusion contains liquid and vapour at room temperature.
	L-only	The inclusion comprises liquid only at room temperature.
Inclusion Generation:	*P (Primary)*	The inclusion was trapped at the time of crystal growth.
	PS (Pseudo-Secondary)	The inclusion was trapped during crystal growth along a healed fracture within the growing crystal.
	S (Secondary)	The inclusion was trapped after crystallisation of the host mineral.

Salinity Considerations

The calculation of the salinity of fluid inclusions is undertaken by comparing microthermometric data with the phase relations in experimentally determined salt-water-gas systems under equilibrium conditions. Some of the systems for which experimental data are available are:

- NaCl-H_2O and NaCl-KCl -H_2O (e.g. Sterner *et al.*, 1988)
- $CaCl_2$ -H_2O and NaCl-H_2O-$CaCl_2$ (e.g. Oakes *et al.*, 1990; Vanko *et al.,* 1988)

For accurate estimations of salinity, microthermometric data must conform to phase relations in the system being used to model the data. For example, in the system NaCl-H_2O (Appendix Figure 3), the eutectic is at -21.2°C. Thus, if this system is to be used to model salinity, then the temperature of first melting (T_{fm}) should approximate to this value. Temperatures significantly below this value indicate that the system NaCl-H_2O is not an appropriate model. The eutectics of the most commonly used model systems are given in Table 1 (Appendix 2).

Another important criterion for accurate salinity estimations in that the phase changes used to estimate salinity occur under equilibrium conditions. Where a phase or state persists at temperatures above or below its stability range it is termed to be "*metastable*". Metastable phase transitions may occur in both liquid-vapour and solid-liquid phase transitions, and cannot be accurately reproduced or modelled using published phase diagrams. For example, inclusions with high liquid:vapour ratios, may on freezing only contain solids (e.g. ice and salt-hydrates) with no vapour phase. On reheating, the vapour phase may not re-emerge until after all the solid phases have melted. In high salinity inclusions, salt-hydrates may persist metastably above their maximum stability temperatures. In either of these situations, phase transitions occur under non-equilibrium conditions and therefore the model systems (measured under equilibrium conditions) do not provide accurate salinity estimates and, if used, tend to underestimate the salinity of the fluid inclusion.

Appendix Table 6 Eutectic temperatures for various salt water systems (From Borisenko 1977 and Shepherd *et al.* 1985).

System	Eutectic temperature (°C)
H_2O-NaCl	-21.2
H_2O-$CaCl_2$	-49.5
H_2O-NaCl-$CaCl_2$	-52.0
H_2O-NaCl-KCl	-23.5
H_2O-$CaCl_2$-$MgCl_2$	-52.2
H_2O-$MgCl_2$	-33.6

THE SYSTEM NaCl-H_2O

Appendix Figure 3 illustrates phase relations in the system NaCl-H_2O under vapour saturated conditions. At salinities <30 wt % NaCl, four of the fields contain solid phases (ice + liquid; hydrohalite + liquid; ice + hydrohalite; and halite + liquid). The cotectics of this system (shown in red on Figure 1; Appendix 2) have been modelled numerically (e.g. Sterner *et al.* 1988) and salinity can be calculated directly from microthermometric observations of T_{ice}, T_{hyd} or T_{halite}. This system is an appropriate model for fluid inclusions that display the following properties:

- $\mathbf{T_{fm}}$ should be ~21°*C*. In dilute solutions, this may be difficult to observe and signs of melting may only be observed at temperatures significantly above this temperature.
- If **ice** is the last phase to melt, no appreciable hydrohalite melting should be observed above T_{fm} , and final ice melting must be in the range -21 to 0°C.
- If **hydrohalite** is the last phase to melt, no appreciable ice melting should be observed above T_{fm}, and the incongruent melting of hydrohalite ($_{Thyd}$) must occur between -21 and +0.1°C.
- If **halite** is the last phase to melt, no appreciable ice melting should be observed above T_{fm}. T_{hyd} should occur at +0.1°C, and halite dissolution (T_{halite}) must occur between +0.1 and 500°*C*.

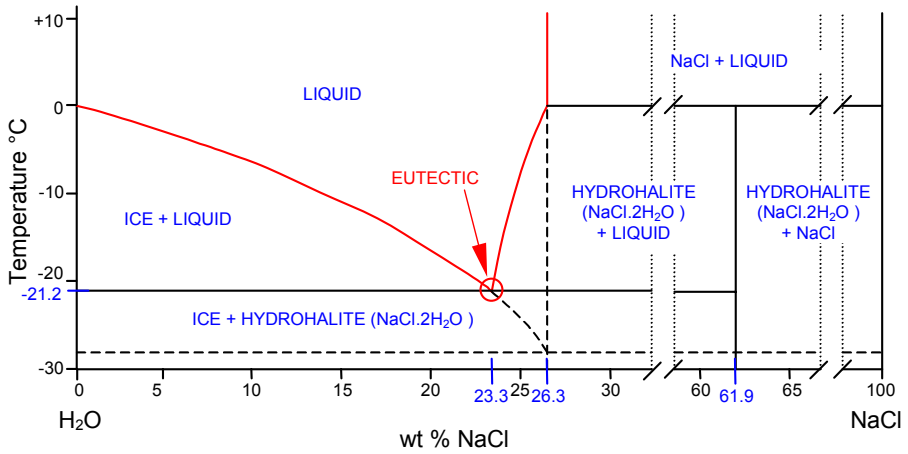

Appendix Figure 3 Temperature-composition plot for the low-temperature part of the system NaCl-H_2O, in equilibrium with vapour, at 1 bar total pressure. Dashed lines represent metastable extensions and meet at the metastable eutectic of ice + NaCl + liquid at ~-28°C.

THE SYSTEM $CaCl_2$-H_2O

The temperature – composition plot for the $CaCl_2$-H_2O binary system resembles that of the NaCl-H_2O system, although the eutectic occurs at –49.8°C, corresponding to approximately 30 wt% $CaCl_2$ in solution and the salt-hydrate phase is antarcticite ($CaCl_2.6H_2O$) rather than hydrohalite. Oakes *et al.* (1990) present experimental data for this system which can be used to derive salinities in terms of wt% $CaCl_2$ from T_{ice} measurements.

THE SYSTEM NaCl-$CaCl_2$-H_2O

The phase diagram in Appendix Figure 4 represents the ternary NaCl-$CaCl_2$-H_2O system. The isotherms on the contoured surface represent the temperature at which the solid + liquid ⇒ liquid phase transition occurs in the presence of a vapour phase (Appendix Figure 3 is a side view of the H_2O-NaCl join). This surface has been modelled numerically (Naden, 1996), which allows salinities to be calculated from measurements of T_{ice}, T_{hyd} and T_{halite}.

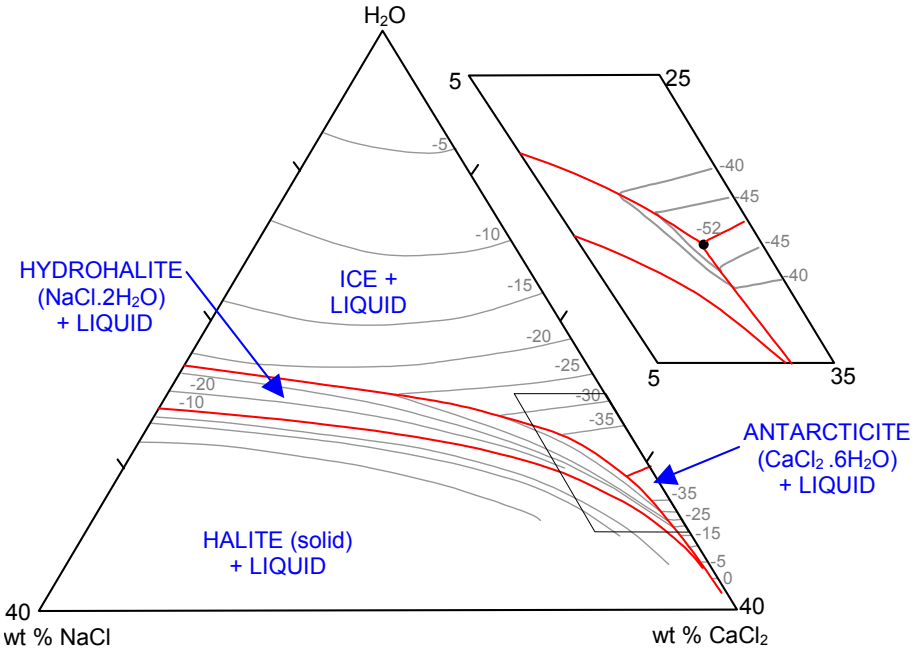

Appendix Figure 4 Phase boundaries, compositions of solid phases, and isotherms in the system H_2O-NaCl-$CaCl_2$ (Redrawn from Shepherd *et al.* 1985, Figures 6.6 and 6.7, based on data in Borisenko, 1977)

For the salinity of a fluid inclusion to modelled using this system, its microthermometric properties should conform to the following rules:

- **T_{fm}** should be in the region of -52°C. In dilute solutions, this may be difficult to observe and signs of melting may only be observed at temperatures significantly above this temperature.
- If **ice** is the last phase to melt, T_{hyd} must be between T_{fm} and -21°C, followed by T_{ice} between T_{hyd} and +0.1°C.
- If **hydrohalite** is the last phase to melt, ice melting must be between T_{fm} and -21°C, followed by T_{hyd} between T_{ice} and +0.1°*C*.
- If **halite** is the last phase to melt, the equilibrium melting path is: hydrohalite + ice + liquid → hydrohalite + liquid → hydrohalite + halite + liquid → halite + liquid → liquid.
  Ice melting must be between T_{fm} and -21°C. In these high salinity fluids, hydrohalite commonly exhibits metastable behaviour and cannot be used in salinity calculations. However, if ice shows equilibrium melting behaviour then T_{ice} can be used in conjunction with T_{halite} to estimate salinity. Finally, T_{halite} must be between T_{hyd} and 500°*C*.

RULES USED IN CALCULATING SALINITY

Two procedures can be used to determine the salinity of a fluid inclusion:

- Only use microthermometric data that conform to the "rules" outlined above. If this approach is used, then a significant number of inclusions will be excluded from the data interpretation. This is particularly significant in the system NaCl-$CaCl_2$-H_2O, where it is not always possible to obtain the paired T_{ice} and T_{hyd} measurements required to estimate NaCl:$CaCl_2$ ratio, and hence salinity.
- The other approach makes several assumptions that enable the maximum amount of data to be included. For example, in an inclusion where T_{fm} indicates the presence of $CaCl_2$, then the systems NaCl-H_2O (T_{ice} >-21°C) and $CaCl_2$-H_2O (T_{ice} <-21°C) provide reasonable estimations of salinities (see Appendix Figure 5 for a comparison of freezing point depression curves for fluids of different salinities and different NaCl:CaCl ratios). Another example would be the case where a solid is observed to melt above the maximum stability limit of hydrohalite. If it is assumed that this phase is halite, then this allows all inclusions that exhibit this phenomena to be included in the procedures for salinity estimation. This approach also reduces several dependant variables (T_{ice}, T_{hyd}, T_{halite}), which may or may not be present in a single inclusion into one -— bulk salinity.

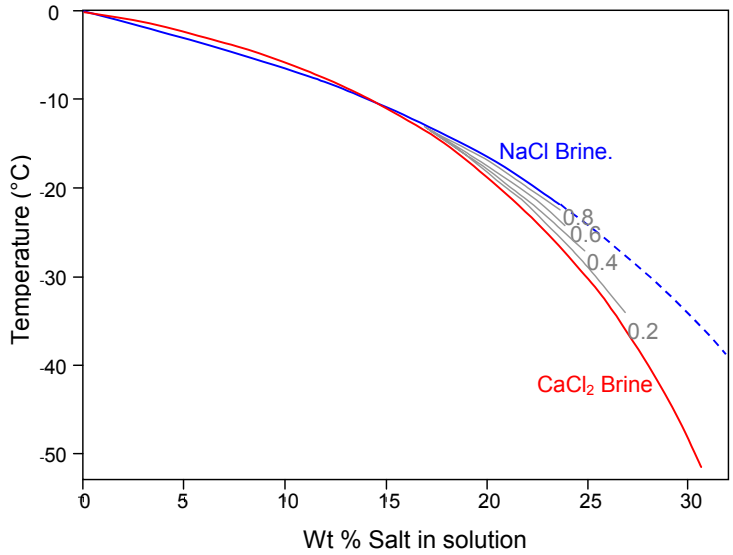

Blue curve: **pure NaCl Brine. The solid portion of this curve indicates the position of the equilibrium cotectic. The dashed portion illustrates extension of the curve to solutions containing > 23.3 wt % NaCl (above which hydrohalite is the last phase to melt).**
Grey curves: **brines of intermediate composition (NaCl/[NaCl+$CaCl_2$] ratio indicated for each curve).**
Red curve: **pure $CaCl_2$ brine.**

Appendix Figure 5 Depression of the freezing point of pure water as a function of the wt % salt in solution. Plotted from data in Oakes et al. (1990).

CATHODOLUMINESENCE MICROSCOPY

Following fluid inclusion microthermometry, the chips extracted from the polished wafers were imaged using a Technosyn 8200 (Mk II) cold-cathode stage mounted on a Nikon optical microscope, with vacuum and beam settings adjusted as required to generate optimum luminescence. Images were captured using a Nikon Coolpix 4500 digital camera attached to the microscope. The CL images were then used to determine the precise location of each analysed fluid inclusion relative to the cement zones present within the sample, and the fluid inclusion data was retrospectively coded with this information.

ULTRAVIOLET MICROSCOPY

In addition, to check for the presence of hydrocarbon-bearing inclusions within the samples, the analysed disks were scanned using an ultraviolet light source attached to an optical microscope. No hydrocarbon-bearing inclusions were observed.

REFERENCES

BORISENKO, A S. 1977. Study of the salt composition of solutions in gas-liquid inclusions in minerals by the cryogenic method. *Soviet Geology and Geophysics,* Vol. 18, 11-19.

GOLDSTEIN, R H, and REYNOLDS, T J. 1995. Systematics of fluid inclusions in diagenetic minerals. *Society of Economic Paleontologists and Mineralogists Short Course,* Vol.31. Tulsa, USA.

NADEN, J. 1996. CalcicBrine 1.5: a Microsoft Excel 5.0 Add-in for calculating salinities from microthermometric data in the system NaCl-CaCl2-H2O. *PACROFI VI Abstracts*, University of Wisconsin.

OAKES, C S, BODNAR, R J, and SIMONSON, J M. 1990. The system NaCl-CaCl2-H2O: I. The ice liquidus at 1 atm total pressure. *Geochimica et Cosmochimica Acta,* Vol.54, 603-610.

ROEDDER, E. 1984. Fluid Inclusions. *Mineralogical Society of America, Reviews in Mineralogy,* Vol.12, ISBN 0-939950-16-2.

SHEPHERD, T J, RANKIN, A H, and ALDERTON, D H M. 1985. A Practical Guide to Fluid Inclusion Studies. (*Blackie, Glasgow and London)* ISBN 0-412-00601-4.

STERNER, S M, HALL, D L, and BODNAR, R J. 1988. Synthetic fluid inclusions: V. Solubility relations in the system NaCl-KCl-H2O under vapour saturated conditions. *Geochimica et Cosmochimica Acta,* Vol.52, 989-1005.

VANKO, D A, BADNAR, R J, and STERNER, S M. 1988. Synthetic fluid inclusions: VIII. Vapour saturated halite solubility in part of the system NaCl-CaCl2-H2O, with application to fluid inclusions from oceanic hydrothermal systems. *Geochimica et Cosmochimica Acta,* Vol. 52, 2451-2456.